1-1-2012

Pax6 is required for the development of the lateral procephalon in tribolium

Qing Luan
Wayne State University,

PAX6 IS REQUIRED FOR THE DEVELOPMENT OF THE LATERAL PROCEPHALON IN TRIBOLIUM

by

QING LUAN

THESIS

Submitted to the Graduate School

of Wayne State University,

Detroit, Michigan

in partial fulfillment of the requirements

for the degree of

MASTER OF SCIENCE

2012

MAJOR: BIOLOGICAL SCIENCES

Approved by

_____

Advisor Date

ACKNOWLEDGEMENTS

I would like to express my special gratitude to my advisor Dr. Markus Friedrich for his support and guidance. Not only the progress of my project work is satisfactory under his supervision, but also the cooperation is pleasant and enjoyable. I was always impressed and influenced by his patience and creativity whenever we encountered obstacles. Also I learnt a crucial feature for a successful scientist from him, that is, how to halter wild imagination to practical plans. His guide always lit up the track ahead and pulled me back when I was going too wide. It was an honor for me to join his group and here I would like to show my highest respect to him.

I hold great thanks to my committee members, Dr. William Branford and Dr. Mark Van Berkum. I highly appreciate their generous support in being my committee members. Their critical reading and revision of my manuscript helped me greatly in improving this thesis work.

Meanwhile, I would like to thank my current and previous colleagues Zahabiya Hussain, Anura Shrivastava, Jasmina Kulacic, Dr. Riyue Bao (Sunny) and Dr. Jason Caravas. I am honestly aware of the importance of a harmonious teamwork and feeling lucky to have them around. Their diligence and passion in both life and work, like the sun in the sky, always makes it cheerful to work and live here, even though I am far away from home. Especially, I am grateful for Zahabiya Hussain and Anura Shrivastava for optimizing the protocol of in situ hybridization, and Harshal Vora for collecting data for control experiments. As well, I appreciate support from our collaborator Dr. Yoshinori Tomoyasu from Miami University, who tested and confirmed our observation.

Also, I would like to express my sincere gratitude to Dr. Edward Golenberg, Dr. Victoria Meller, Dr. Xiang-Dong Zhang and Dr. Miriam Greenberg for their training, advice and support. I would like to thank the staff of the department for all the daily support and assistance, especially Ms Rose Priest, who always helps me deal with complex paperwork with patience and smile. I would like to thank all my friends in Biological Sciences Department and at Wayne State University for accompanying me, my friends all over the world for mental comfort.

At last, I would like to thank my family, my parents and my wife, for being healthy and happy as their support and understanding. They make me just me.

Thank you so much! I love you all!

TABLE OF CONTENTS

LIST OF FIGURES

LIST OF TABLES

LIST OF ABBREVIATIONS

General

AP: alkaline phosphatase

BSA: bovine serum albumin

CDS: coding sequence

CNS: central nervous system

DIG: digoxygenin

dsRNA: double-stranded RNA

BCIP: 5-bromo-4-chloro-3'-indolyphosphate p-toluidine salt

DABCO: 1,4-diazabicyclo[2.2.2]octane

EGFP: enhanced green fluorescent protein

GA-1: Georgia-1

KD: knockdown

NBT: nitro-blue tetrazolium chloride

PBS: phosphate buffered saline

PBT: phosphate buffered saline plus Tween-20

RNAi: RNA interference

RT-PCR: reverse transcription polymerase chain reaction

WT: wild type

Genes

dac: dachshund

disco: disconnected

ey: eyeless

ind: intermediate neuroblast defective

toy: twin of eyeless

wg: wingless

Anatomy

AL: antennal lobe

ant: antenna

CB: central body

dpn: dorsal protocerebral neuroectoderm

hlo: head lobe

int: intercalary

lbr: labrum

lpc: lateral procephalon

man: mandible

mpn: medial protocerebral neuroectoderm

vpn: ventral protocerebral neuroectoderm

mpc: medial procephalon

MSB: mushroom body

mx: maxilla

pc: protocerebrum

pgz: posterior growth zone

pne: protocerebral neuroectoderm

sep: subesophageal ganglion

sto: stomodeum

vp: visual primordium

Chapter 1: Introduction

PAX6 transcription factor genes are characterized by two DNA binding domains: a paired-domain (PAX) and a homeodomain (Callaerts et al., 1997). These developmental regulators stand out by being crucial for eye development in numerous vertebrates and invertebrates (Callaerts et al., 2006; Hanson, 2003). In mouse, mutations in *Pax6* lead to complete loss of eyes (Hill et al., 1991). In humans, mutations in *Pax6* are the molecular cause of the *Aniridia* syndrome, characterized by failed eye development in homozygous patients (Niederfuhr et al., 1998; Quiring et al., 1994). Remarkably, *Pax6* induces ectopic eye formation in both vertebrates and invertebrates when misexpressed (Chow et al., 1999; Czerny et al., 1999; Halder et al., 1995). The necessity and sufficiency for eye development have led to *Pax6* being considered a master gene regulator of eye development. The functional conservation is also reflected at the sequence level. The sequence identity in the PAX domain and homeodomain between mouse and *Drosophila* amounts to over 80% and 94%, respectively.

Consistent with its pivotal role in eye development, *Pax6* is expressed in the developing eyes of many different organisms (Callaerts et al., 1997). However, in most cases the expression of *Pax6* also includes other areas such as elements of the central nervous system (CNS) (Martin-Duran et al., 2012), where its function is not yet fully understood. A recent study revealed that *Pax6* is essential and sufficient for neuroectoderm fate determination in primates but not in rodents (Zhang et al., 2010), suggesting evolutionary diversification of specific functions. *Pax6* is also expressed in

the pancreas of mouse, where *Pax6* mutations are linked with diabetes (Ashery-Padan et al., 2004).

Two distantly linked orthologs of *Pax6* are present in the genome of *Drosophila melanogaster* (Bopp et al., 1986; Czerny et al., 1999): *eyeless* (*ey*) and *twin of eyeless* (*toy*). *ey* was shown to be expressed in the developing eye-imaginal disc, CNS and insulin-secreting neurons in remarkable correspondence with the expression domains in mouse (Clements et al., 2008). *toy* is expressed in many domains spatially overlapping with *ey* (Czerny et al., 1999). However, paralog-specific domains exist as well, such as that of *toy* in the anterior early blastoderm embryo (Czerny et al., 1999). Hypomorphic alleles of *ey* or *toy* lead to eye-depletion in adult flies (Czerny et al., 1999; Hauck et al., 1999; Xu et al., 1999). Strong mutants of *ey* or *toy* cause reduction of the adult head capsule, due to the perturbed development of structures derived from the eye imaginal disc (Kronhamn et al., 2002).

The development of the Bolwig's organ, the visual organ of the *Drosophila* larva, is not affected by the loss of *ey* and *toy* (Suzuki and Saigo, 2000). Given the lower complexity and smaller size of the head region in the *Drosophila* larvae, it has been proposed that *Pax6* functions as a regional patterning gene which modulates the lateral head development, rather than a visual organ-specific determining gene. According to this model, the widespread occurrence of adult eye phenotypes are the consequence of broader head patterning defects, which center around the position of the peripheral visual organs. The strong bias for ectopic eye development in *Pax6* misexpression

experiments, however, favors the idea of *Pax6* as a master gene regulator of visual organ induction.

Further evidence of a regional patterning function of *Pax6* in the developing insect head has been obtained from experiments in the red flour beetle *Tribolium castaneum*. Like *Drosophila*, the *Tribolium* genome harbors orthologs of *ey* and *toy* (Yang et al., 2009a). Unlike in *Drosophila*, however, the visual organs of both the larva and adult were found to be sensitive to reduction of *ey* and *toy* activity by RNA interference in *Tribolium* (Yang et al., 2009a). The sensitivity of the *Tribolium* larval eyes is consistent with the overlapping expression of *ey* and *toy* in the head lobes, the lateral compartments of the anterior procephalon of the early developing head (Fig. 1). While the single knockdown (KD) of *ey* causes mild eye reduction at low penetrance (~20%), single KD of *toy* leads to a stronger eye depletion phenotype and higher penetrance (58%). When *ey* and *toy* are targeted in combination by RNAi, the eye depletion phenotype is synergistically enhanced (90% penetrance), uncovering the redundant regulation of processes necessary for normal larval eye development by the two *Pax6* paralogs (Yang et al., 2009a).

In addition to the larval eyes, the larval head capsule is affected in combinatorial *ey* and *toy* KD *Tribolium* as indicated by the loss of specific dorsal bristle elements and an overall reduction of the lateral head capsule in severe cases (Posnien et al., 2011; Yang et al., 2009a). The origins of these defects and their spatial dimensions have not yet been elucidated in detail.

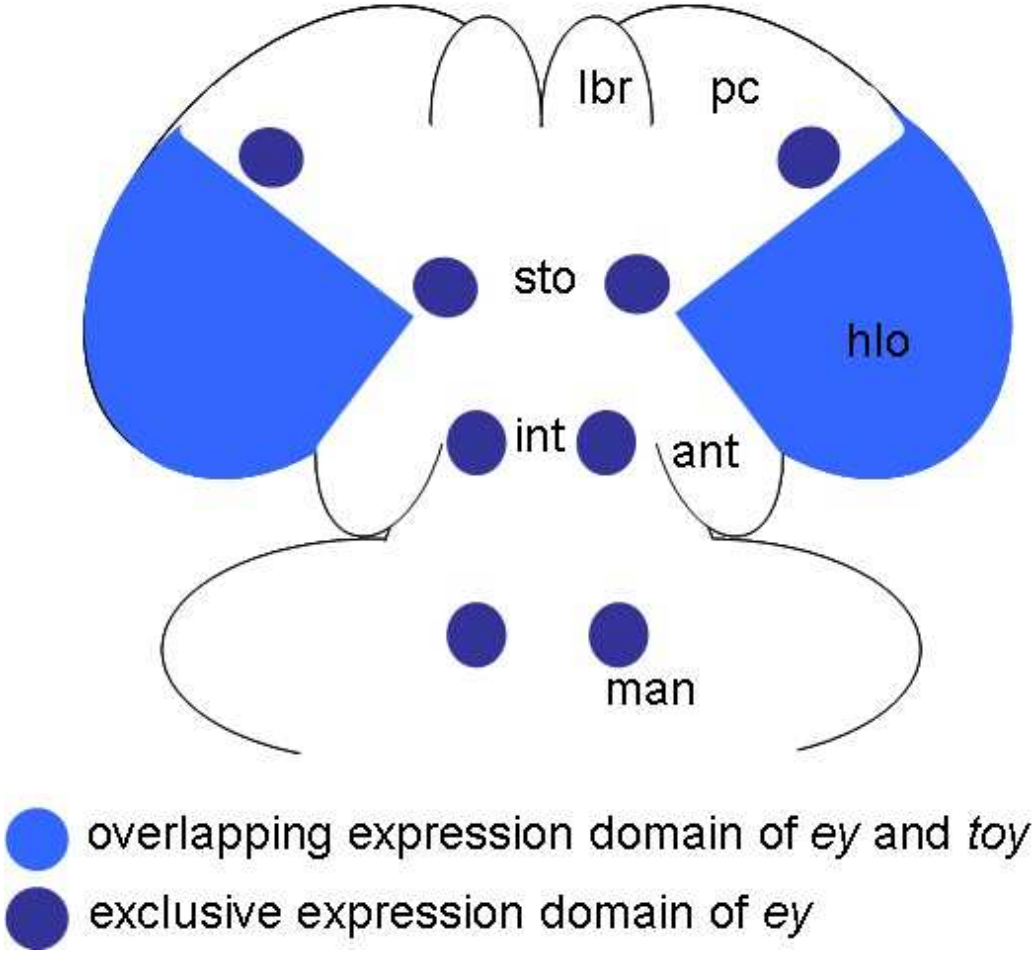

Fig. 1: Schematic comparison of *ey* and *toy* expression in the embryonic head of Tribolium at germband extension complete stage.

The image was drawn based on previous findings (Yang et al., 2009a). Anterior is to the top. The blue regions represent the overlapping expression domains of *ey* and *toy* in the ventral portion of the head lobes. The violet regions represent exclusive *ey* expression domains in median cell clusters of the head segments.

Abbreviations: lbr: labrum; pc: protocerebrum; sto: stomodeum; int: intercalary; hlo: head lobe; ant: antenna; man: mandible.

Here, we describe the results of studying the role of the *Pax6* genes *ey* and *toy* in the embryonic head of *Tribolium* in depth. Our results demonstrate that *Pax6* is required for the development of a large region of the lateral head. This region, which we refer to as the lateral procephalon and which seems to correspond to much of the morphologically defined head lobe compartments, gives rise to parts of the larval brain and the dorsal head cuticle in addition to the larval eyes. This finding lends further support to the idea that *Pax6* acts as a regional specification gene.

Chapter 2: Methods and materials

2.1. Animals

The wild type *Tribolium castaneum* used in this work was from the Georgia-1 (GA-1) strain and the pBac{3XP3-EGFP} transgenic line (Lorenzen et al., 2003). The cultures were maintained as previously described (Liu and Friedrich, 2004). All analyses were done with 1st instar (L1) larvae.

2.2. RNA interference

Parental *RNAi* procedures were performed as described (Bucher et al., 2002; Posnien et al., 2009). For adult parental *RNAi*, adult females were isolated for several days before injection to reduce the number of older, normally developing eggs. For injection, animals were anaesthetized by CO2 and immobilized on tape. Templates for dsRNA *in vitro* transcription were amplified by RT-PCR that introduced T7 polymerase promoter sites through 5'-end primer extension. cDNA was generated by

reverse transcription of total RNA from wild type GA-1 *Tribolium* pupae. The Megascript T7 reagent kit (Ambion) was used for *in vitro* transcription of dsRNA. The dsRNA against *Tribolium ey* (TC008176) targeted the homeodomain-encoding region between nucleotides 401 and 1123 of the coding sequence (CDS). The dsRNA against *Tribolium toy* (TC007409) corresponded to the homeodomain-encoding region between nucleotides 701 and 1374 in the CDS. Control-injection dsRNA consisted of the whole CDS of the *egfp* gene (~720bp). Primer sequences are included in Table 1.

For pupal parental *RNAi*, day 2 or day 3 female pupae were immobilized with glue on slides. The dsRNA for *ey* targeted the region between nucleotides 181-872 (encoding both the PAX domain and homeodomain) of the *ey* CDS. The dsRNA for *toy* (~850bp) targeted a CDS region encoding both the PAX domain and homeodomain. For *ey/toy* double KD, 1ug/ul *ey* and 1ug/ul *toy* dsRNA were co-injected into the pupae.

2.3. Cuticle pattern analysis

The standard pattern of sensilla in the dorsal head of WT GA-1 L1 larvae was established by scoring 160 samples (Fig. 2a). The threshold condition for including sensilla in the standard pattern was the presence in 95% or more of the WT individuals sampled. Specific sensilla were named by adopting the nomenclature of Schinko et al. (Schinko et al., 2008) when possible or introducing new terms as described in Table 2.

2.4. Whole mount in situ hybridization on embryos

primers for dsRNA	
name	sequence
Tcas_ey_forward	AAAAAGAGCAAACGTCCCAG
Tcas_ey_reverse	TCGGACTTTCCCTTTGTTGC
Tcas_toy_forward	ACAAGCTGCGGATGTTCAAC
Tcas_toy_reverse	AGCCCTCGAGTTGTATGAAG
primers for probe	
name	sequence
Tcas_wg_forward	GTCAAGAATGTAAATGCCACG
Tcas_wg_reverse	GCACTTCACTTCACAGCACC
Tcas_disco_forward	ATGTCACCTAACCATCGCC
Tcas_disco_reverse	CTTTGTCGCAAAACGTC
Tcas_ind_forward	ATGAACATGTCACGATCATTC
Tcas_ind_reverse	TAATGACAATGGTCATC

Table 1: Primer sequence for dsRNA and probe generation.

Abbre	Full name	Correspond in Schinko's model
AVB	anterior vertex bristle	anterior vertex bristle
AVA	anterior vertex alveolus*	close to anterior vertex bristle
AVS	anterior vertex seta	anterior vertex triplet
ABB	antenna basis bristle	antenna basis bristle
ABA	antenna basis alveolus	close to antenna basis bristle
MVB	median vertex bristle	median vertex bristle
DMA	dorsomedian alveolus	close to dorsomedian alveolus
DMB	dorsomedian bristle	dorsomedian bristle
LVS	lateral vertex seta	ventral vertex triplet
PVB	posterior vertex bristle	posterior vertex bristle
PVA	posterior vertex alveolus	close to posterior vertex bristle
RB	row bristle	row bristle
BR	bell row	bell row

Table 2: Nomenclature of sensillum pattern on the dorsal head.

The nomenclature of sensillum pattern is adopted from Schinko's model (Schinko et al., 2008). The position of the sensilla refers to Fig. 2a.

* The usage of the term "alveolus" refers to A Dictionary of Entomology, second edition, Gordon Gordh and David Headrick, 2011, ISBN: 9780643097841

Whole mount *in situ* hybridization was performed as previously described (Friedrich and Benzer, 2000). Templates for probe *in vitro* transcription were amplified by RT-PCR by introducing a T7 polymerase promoter site to the 5'-end of the reverse primer. cDNA was generated by reverse transcription of total RNA from WT GA-1 *Tribolium* pupae. The T7 polymerase (Ambion) was used for *in vitro* transcription of probes and the probes were labeled with digoxygenin (DIG) by adding DIG RNA labeling Mix (Roche) to the reaction. Anti-DIG-AP fab fragment (Roche) was used for detection and NBT/BCIP reaction was used for staining. The probe for *wingless* (*wg*) (TC014084) targeted the region between nucleotides 734 and 1248 of the CDS. The probe for *disconnected* (*disco*) (TC001693) targeted the region between nucleotides 499 and 1266 of the CDS. The probe for *intermediate neuroblast defective* (*ind*) (TC006888) targeted the whole CDS. Primer sequences are included in Table 1.

2.5. Analysis of morphogenesis, cell proliferation and cell death

0-36 hour old embryos were collected and fixed in 10% formaldehyde/PBS. Cellular tissue organization was visualized by labeling with Alexa Fluor 633-phalloidin (Molecular Probes, Cat#A22284). Embryos were blocked in blocking buffer (1mg/ml BSA/PBT) at room temperature for 1hr, followed by overnight incubation in 1:50 diluted Alexa Fluor 633-phalloidin/blocking buffer at 4°C. Mitotic and apoptotic cells were visualized by staining with propidium iodide. Embryos were treated with 400ug/ml RNaseA at room temperature for 1hr, followed by overnight incubation in 5ug/ml propidium iodide at 4°C. All incubation procedures were carried out in

Eppendorf tubes wrapped in aluminum foil for protection from light. The stained embryos were cleared and mounted in 2.5% DABCO/70% glycerol/PBS.

2.6. Imaging

To inspect or image larval cuticle morphologies, larvae were collected in mineral oil and mounted live, dorsal side up. Nomarski microscopic images were taken on a Zeiss Axioskope and with a RT Spot camera and software (Diagnostic Instruments). Confocal imaging was taken with a Leica TCS-SP2 laser scanning confocal microscope. Images were processed using Adobe Photoshop CS4.

Chapter 3: Results

3.1. Pax6 knockdown causes a range of larval head cuticle deformations

Previous studies reported the posterior reduction and dorsal bristle pattern defects in the L1 head capsule of *Pax6* KD *Tribolium*, in addition to the larval eye depletion phenotype (Posnien et al., 2011; Yang et al., 2009a), indicating a broader patterning role for *Pax6* in the developing embryonic head of *Tribolium*. To further test this possibility and determine the putative *Pax6*-sensitive region, we examined a large sample of L1 cuticles in larval offspring of females co-injected with 1 ug/ul *toy* and 2 ug/ul *ey* dsRNA. For the remainder of this report, we will refer to the combinatorial KD of *ey* and *toy* as *Pax6* KD.

The larvae of *Tribolium* are characterized by a well-developed head capsule, which is furnished with four larval eye clusters, two on each side. The visual organs are

prominent in WT animals as they consist of pigment-enriched photoreceptors (Fig. 2a). In a total of 356 examined *Pax6* KD larvae, over 80% suffered from complete loss of at least one eye (Fig. 2b and e). The remainder suffered from unilateral loss or reduction of photoreceptor clusters (Fig. 2b). Very few larvae (3 out of 356) had normal eyes on both sides. In addition to the larval eye defects, 30% of the larvae suffered from severe reduction of the head capsule (Fig. 2c, d and e). This was associated with deep folds in the lateral head capsule (Fig. 2c and d) and an extension of a neck-like groove that spanned across the posterior vertex of dorsal head (Fig. 2d). An additional 40% of the *Pax6* KD larvae exhibited milder forms of head capsule reduction (Fig. 2e). Overall, eye and cuticle defects were frequently present in asymmetric unilateral patterns (Fig. 1b, c and f). However, comparison of the average frequency of defects observed on the right side of the head cuticle versus the left revealed no difference (Fig. 2e). Finally, larval eye phenotypes were more frequent than the additional dorsal head cuticle reduction, indicating a higher sensitivity of the peripheral visual system or of the corresponding area to the reduction of *Pax6* levels. The same cuticle and larval eye phenotypes resulted from pupal parental *RNAi* (see Methods and Materials 2.2) with different *ey/toy* dsRNAs (Fig. 3), reducing the possibility that our observations are the result of off-target effects. The injection of 3ug/ul *egfp* dsRNA did not affect the development of *Tribolium.*

In a small number of individuals, a unilateral appendage-like protrusion was observed in the anterior lateral head region where larval eyes normally localize (2 out of 356 *Pax6* KD GA-1 larvae and 3 out of 60 *Pax6* KD 3XP3-EGFP larvae) (Fig. 2g).

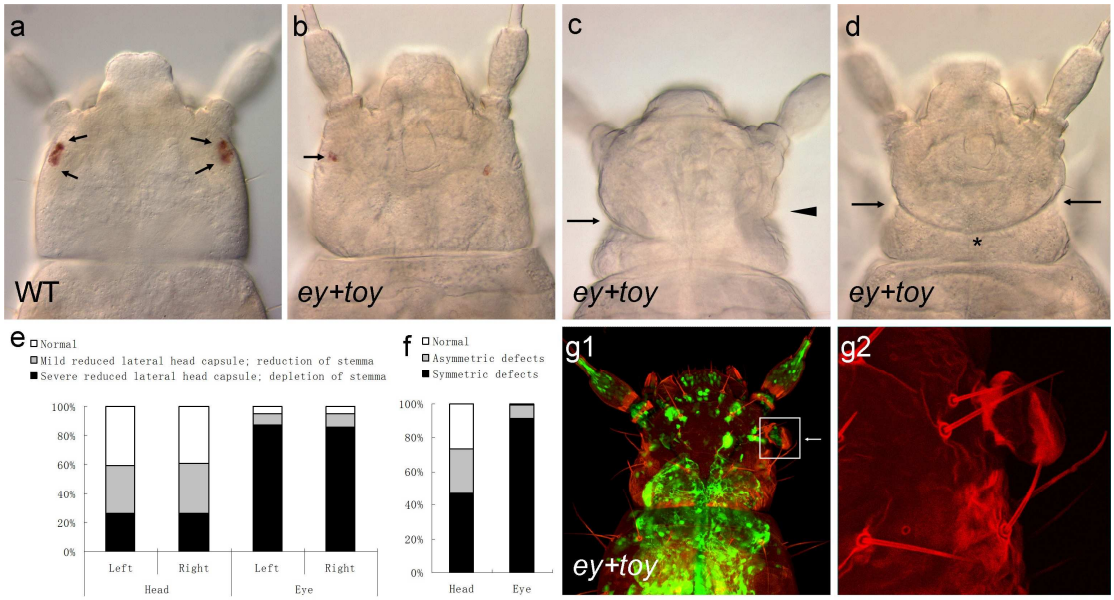

Fig. 2: *Pax6* knockdown phenotypes in the dorsal head of *Tribolium* larvae.

(a-h) Dorsal view of the head of larvae. Anterior is to the top. (a) WT GA-1. Normal larval eye is composed of two clusters of pigmented photoreceptors (arrows). (b-d) *Pax6* KD phenotype of GA-1. (b) *Pax6* KD larva showed only one reduced cluster of pigmented photoreceptors (arrow). (c-d) *Pax6* KD larva showed complete loss of larval eyes and reduced lateral head capsule (arrows indicate severe reduction and arrowhead indicates mild reduction). When both sides of lateral head capsules were reduced, a 'neck'-like groove (asterisk in Fig. 2d) was left on the posterior vertex of dorsal head. (e) Penetrance of head capsule and eye defective phenotypes (n=356). Mild defects include reduced larval eye (arrow in Fig. 2b) and mild reduction of lateral head capsule (arrowhead in Fig. 2c). Severe defects include complete loss of larval eye and severe reduction of lateral head capsule (arrow in Fig. 2c and d). (f) Proportion of asymmetric and symmetric defects (n=356). (g) Appendage-like structure in the ocular compartment of *Pax6* KD larva (2 out of 356 *Pax6* KD GA-1 larvae and 3 out of 60 *Pax6* KD 3XP3-EGFP larvae). The green signal represents the 3XP3-EGFP expression. The red fluorescence represents the auto-fluorescence of the cuticle. Fig.2g2 is an enlargement of the inset in Fig. 2g1.

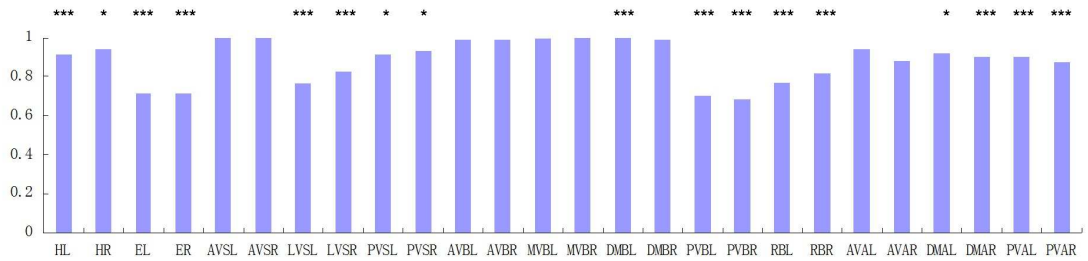

Fig. 3: Statistical graph of the phenotypic penetrance of *Pax6* knockdown larvae generated by pupal parental RNAi and dsRNA targeting PAX and HOX domain.

See methods and materials for detailed procedure. n=136. Compared with the control group in Fig. 4c. Single asterisk indicates $p<0.05$; triple asterisk indicates $p<0.01$.

Abbreviations: H: head; E: eye; AVB: anterior vertex bristle; AVA: anterior vertex alveolus; AVS: anterior vertex seta; ABB: antenna basis bristle; ABA: antenna basis alveolus; MVB: median vertex bristle; DMA: dorsomedian alveolus; DMB: dorsomedian bristle; LVS: lateral vertex seta; PVB: posterior vertex bristle; PVA: posterior vertex alveolus; RB: row bristle; BR: bell row. A suffix letter L or R indicates left or right, respectively

On closer examination, no specific hallmark structures of other appendages, such as bristles or sensilla, could be detected on these protrusions. However, two circumferential autofluorescent areas, reminiscent of the joint sockets in other body appendages, were noted (Fig. 2g).

Further analysis of the head morphology of strongly affected individuals did not reveal any conspicuous defects in the mouth parts or the ventral head. Examination of unhatched eggs (<3%) did not reveal any severely deformed embryos, as might be expected in the case of strong embryonic-lethal patterning phenotypes. Further consistent with the viability of *Pax6* KD animals, strongly affected L1 larvae were able to proceed into the L2 stage.

3.2. Pax6 knockdown defects are restricted to the dorsal lateral and posterior regions of the larval head capsule

Considering the evidence of differential sensitivity of larval head patterning to *Pax6* reduction, we carried out a more comprehensive quantitative analysis of the phenotype by investigating the sensillum pattern of first instar larvae. A total of 356 *Pax6* KD offspring larvae were examined. *egfp* dsRNA control injection did not affect sensilla of larvae (Fig. 4a). In the *Pax6* KD larvae, the posterior vertex bristles and row bristles were most frequently missing (>80%), followed by lateral vertex setae and antenna basis bristles (>60%) (Fig. 4b and c). The posterior vertex setae and alveoli also showed significant reduction in *Pax6* KD larvae but at a lower percentage (>25%) (Fig. 4b and c). Sensilla of the anterior and medial region were missing in an

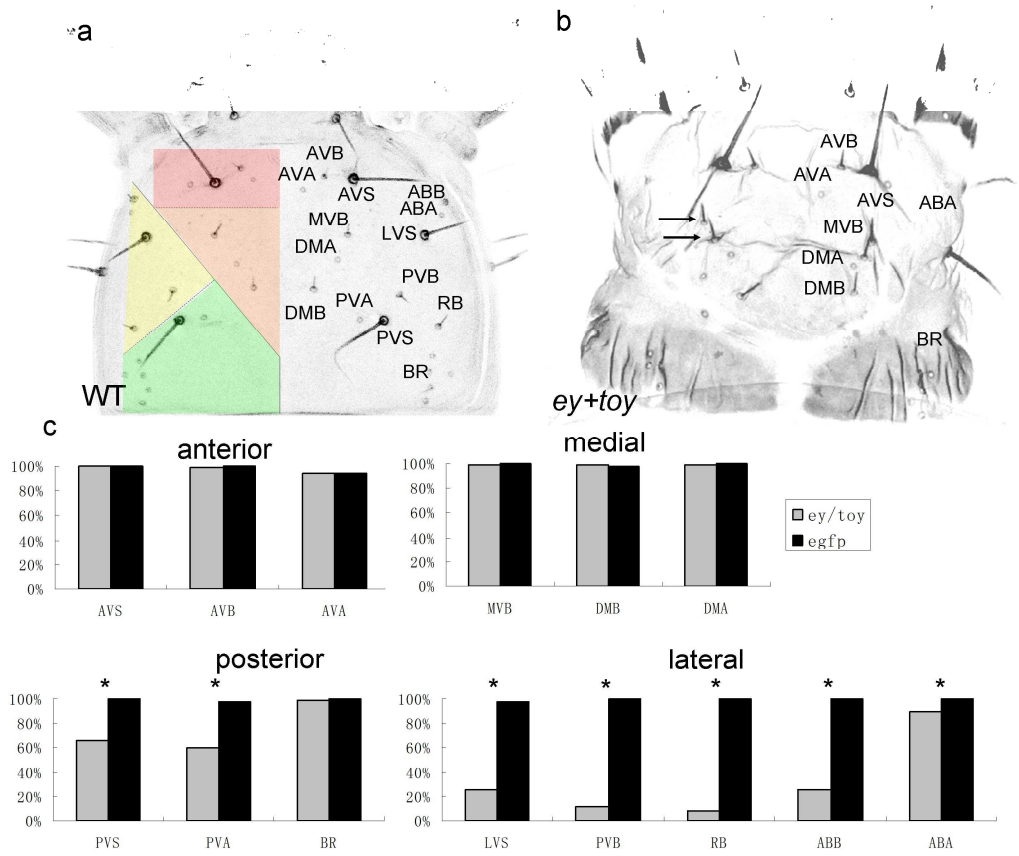

Fig. 4: Bristle pattern analysis of *Pax6* knockdown head cuticle phenotypes in *Tribolium* larvae.

(a, b) A typical example of dorsal sensillum loss in *Pax6* KD larvae. (a) WT GA-1. The straight line represents the epicranial suture and spotted lines represents putative boundaries of different regions of the dorsal head. Different regions are colored as following: red-anterior, orange-medial, yellow-lateral, green-posterior. (b) A representative sensillum pattern of *Pax6* KD GA-1. Lateral sensilla are missing (compare with Fig. 3a) and medial sensilla are duplicated (arrows). (c) Statistical graph of the sensilla (n= 356). The bars represent sensilla on the right side. The defects did not show asymmetric bias. The control group was 3ug/ul *egfp* KD larvae (n=55). Asterisk indicates $p<0.01$.

Abbreviations: AVB: anterior vertex bristle; AVA: anterior vertex alveolus; AVS: anterior vertex seta; ABB: antenna basis bristle; ABA: antenna basis alveolus; MVB: median vertex bristle; DMA: dorsomedian alveolus; DMB: dorsomedian bristle; LVS: lateral vertex seta; PVB: posterior vertex bristle; PVA: posterior vertex alveolus; RB: row bristle; BR: bell row.

insignificantly small number of *Pax6* KD larvae (<10%, p-value>0.05) (Fig. 4b and c). However, we observed evidence of bristle transformation or duplication in most of the sampled *Pax6* KD specimens (KD 98.3% vs. control 0%) (arrows in Fig. 43b).

Spatial survey of the data revealed that *Pax6* KD sensitive cuticle elements were restricted to the lateral and posterior region of the larval dorsal head, separated by the Y-shaped epicranial suture of the medial region (Fig. 4a, c). Previous work suggests that the epicranial suture represents the junction of the procephalic and labral head compartments (Posnien and Bucher, 2010). We therefore concluded that the *Pax6* KD affected a large region of the embryonic procephalon, consistent with the overlapping expression domains of *ey* and *toy* in the lateral lobes of the developing embryonic head of *Tribolium* (Fig. 1) (Yang et al., 2009a).

3.3. Brain defects in Pax6 knockdown larvae

Since the procephalic neuroectoderm also includes the precursor tissue of the protocerebrum, we reasoned that the *Pax6* KD might also be associated with developmental defects in supraesophageal ganglia. To probe for the impact of *Pax6* KD on the larval brain, we performed *Pax6* KD in 3XP3-EGFP transgenic *Tribolium castaneum*, which express EGFP in the glial cells (Pavlopoulos et al., 2004; Posnien et al., 2011). In WT *Tribolium* L1 larvae, the brain divides into hemispheres, with glia cells surrounding the two major inner neuropils in each hemisphere (Fig. 5a). The anterior bilateral neuropil pair constitutes the round-shaped antennal lobes (AL) (Fig. 5a, asterisk), which are derived from the deutocerebrum. The posterior major neuropils

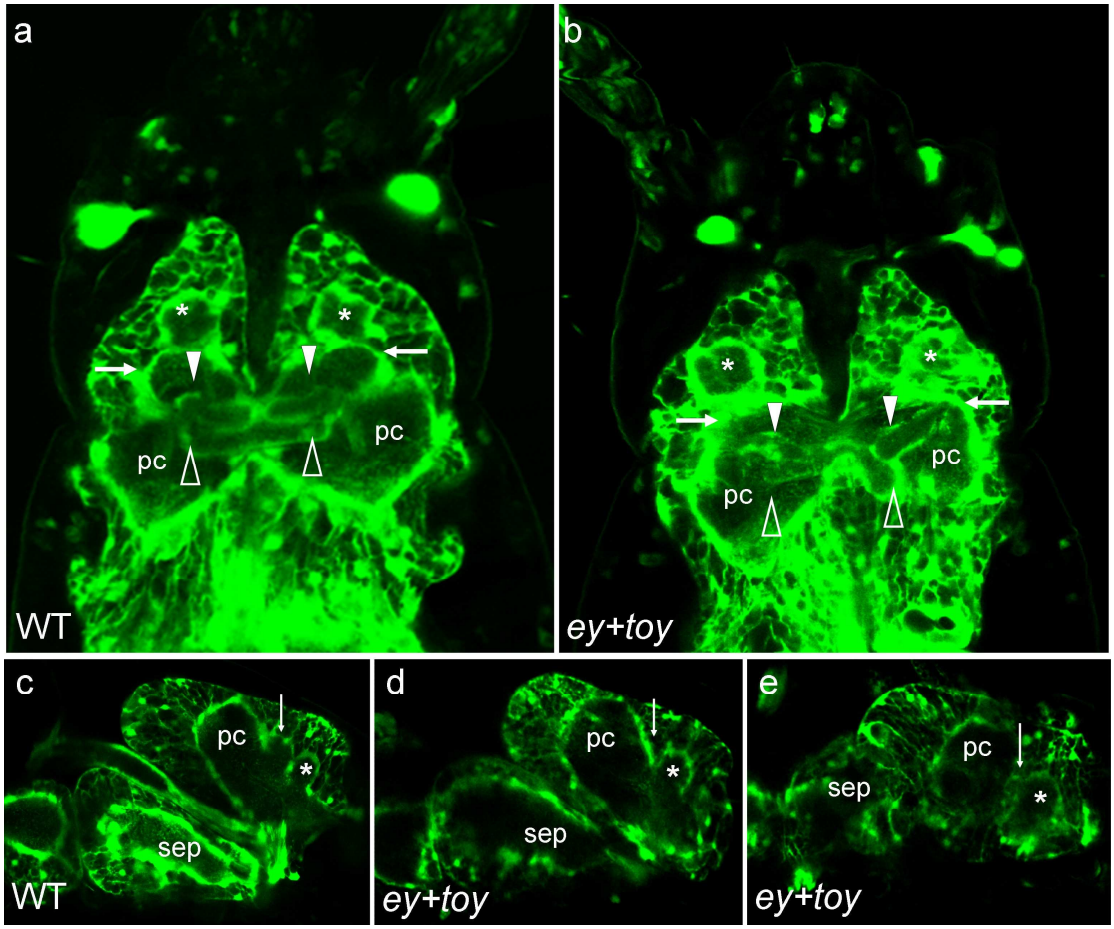

Fig. 5: Brain phenotypes in *Pax6* knockdown *Tribolium* larvae.

(a, b) Dorsal view of 3XP3-EGFP *Tribolium* L1 larval head. The green signal represents EGFP expression in the glia cells. Anterior is to the top. (a) WT 3XP3-EGFP larva. The intermediate protocerebral lobe is marked by arrows. The median lobe of the MSB is marked by white arrowheads and the CB is marked by open arrowheads. The AL is marked by an asterisk. (b) *Pax6* KD phenotype of 3XP3-EGFP larva. The arrows indicate the reduced intermediate protocerebral lobes. The white arrowheads indicate the separated median lobes of the MSB. The open arrowheads indicate the CB. The asterisk indicates the AL. (c-e) Lateral view of 3XP3-EGFP *Tribolium* L1 larval brain. Anterior is to the right. (c) WT 3XP3-EGFP larva. The arrow indicates the intermediate protocerebral lobe, flanked by the greater wing of the protocerebral lobe (pc) and the AL (asterisk). (d) Mild *Pax6* KD phenotype of 3XP3-EGFP larva. The arrow indicates that the intermediate protocerebral lobe is missing. (e) Severe *Pax6* KD phenotype of 3XP3-EGFP larva. The arrow indicates a gap between the protocerebral neuropil and the AL.

Abbreviations: pc: protocerebrum; sep: subesophageal ganglion; AL: antennal lobe; MSB: mushroom body; CB: central body.

are butterfly-shaped and represent the protocerebral lobes (Fig. 5a).

The overall morphology and size of the supraesophageal ganglion were not dramatically altered in *Pax6* KD larvae compared with WT (Fig. 5b). However, the protocerebral neuropils generally lost their butterfly-shaped morphology in *Pax6* KD larvae (Fig. 5b), indicating developmental defects. Closer inspection confirmed that the intermediate wings of the protocerebral neuropils were frequently reduced or missing (14 out of 17 dorsally and 5 out of 7 laterally, Fig. 5b and f). In severe cases, a notch was formed laterally between the protocerebral neuropil and the AL (3 out of 7, Fig. 5g). Similar defects were observed in the developing neuropils of *Pax6* KD embryos, where the protocerebral neuropils was separated by nucleated cells (Fig. 6). No abnormalities were observed in the AL of the same specimen.

In *Drosophila*, *ey* and *toy* have been shown to be essential for mushroom body (MSB) development (Furukubo-Tokunaga et al., 2009; Kurusu et al., 2000). Since these compartments of the brain can also be effectively visualized in the 3XP3-EGFP transgenic *Tribolium* (Posnien et al., 2011), we studied development and morphology of the MSB and the central body (CB) in *Pax6* KD larvae. In WT larvae, the CB and the median lobes of the MSB are outlined by glia scaffolds (Fig. 5a). The CB spans across the midline of the supraesophageal ganglion (Fig. 5a). The two median lobes of the MSB are located anteriorly adjacent to the CB and contact each other at the midline of the supraesophageal ganglion (Fig. 5a). Laterally, the peripheral flanks of the CB and mushroom bodies extend to a similar degree. In *Pax6* KD larvae, the median lobes of the MSB were separated by a consistent interspace (10 out of 12, Fig. 5b). This

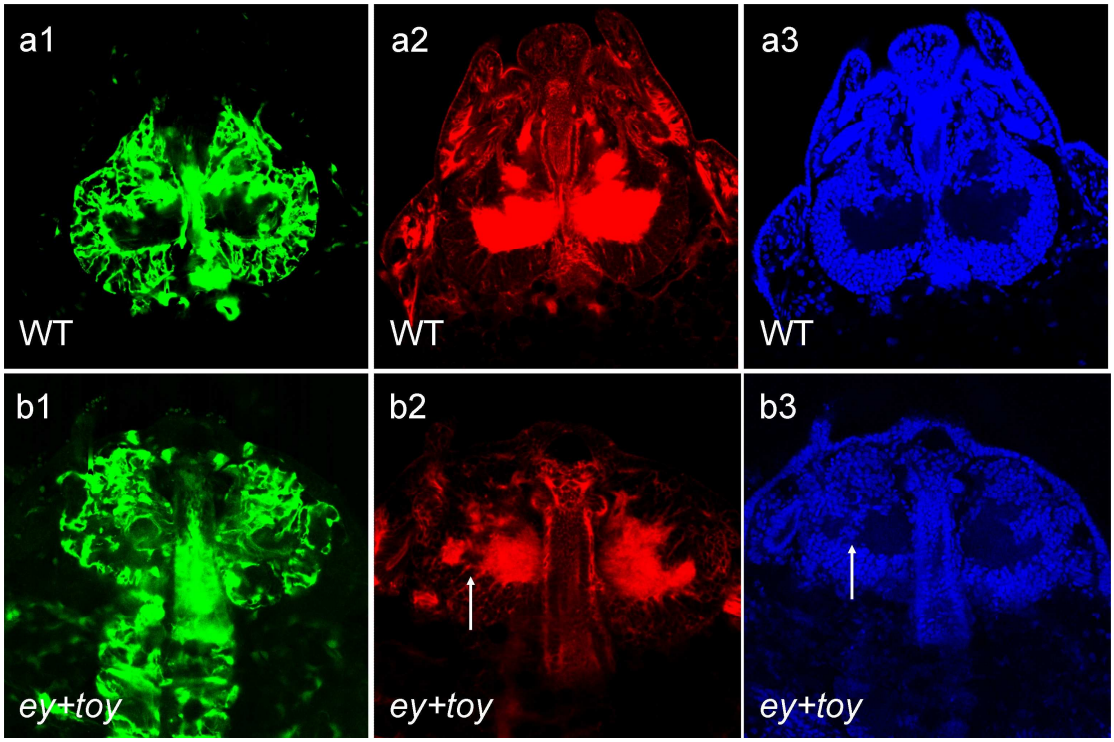

Fig. 6: Defective protocerebral neuropils in *Pax6* knockdown embryos.

(a) Wild type 3XP3-EGFP prenatal embryonic head. The green panel is the signal for 3XP3-EGFP, marking the glia cells. The red panel is the signal for Alexa Fluor 633-phalloidin, marking the neuropils. The blue panel is the signal for propidium iodide, marking the nuclei. (b) *Pax6* KD phenotype of 3XP3-EGFP prenatal embryonic head. The arrow indicates a gap within the neuropil that is filled by nucleated cells.

interspace appeared to be occupied with extra glia cells (Fig. 7).

Examination along the dorsal-ventral axis did not reveal obvious disorientation of the MSB, and the total length of the median lobes including the glia was comparable to the CB, suggesting that the size of the MSB median lobes was reduced. No notable differences in the morphology of the CB could be detected in *Pax6* KD larvae compared to WT. Taken together, the abnormal morphologies of the protocerebral neuropils and MSB median lobes in *Pax6* KD animals further supported the model that *Pax6* is required for the development of a larger area of the *Tribolium* procephalon than the visual primodium.

3.4. Pax6 knockdown is associated with early reduction of the lateral embryonic head

The combined loss of peripheral and central components of the procephalic head compartment in *Pax6* KD animals without evidence of a correlated compensatory increase of other head areas suggested failed tissue specification or precursor tissue expansion during embryonic head development. To test this, we investigated the morphogenetic organization of the early developing head by phalloidin labeling of F-actin in embryonic cells. In WT embryos at the late germband extension stage (staging by the extent of labrum extension), the procephalic compartment consists of the median protocerebrum and the lateral head lobes. In reference to the embryonic longitudinal body axis, the anterior head lobe constitutes the neuroectodermal precursor tissue of the lateral procephalon and the posterior head lobe that of the visual

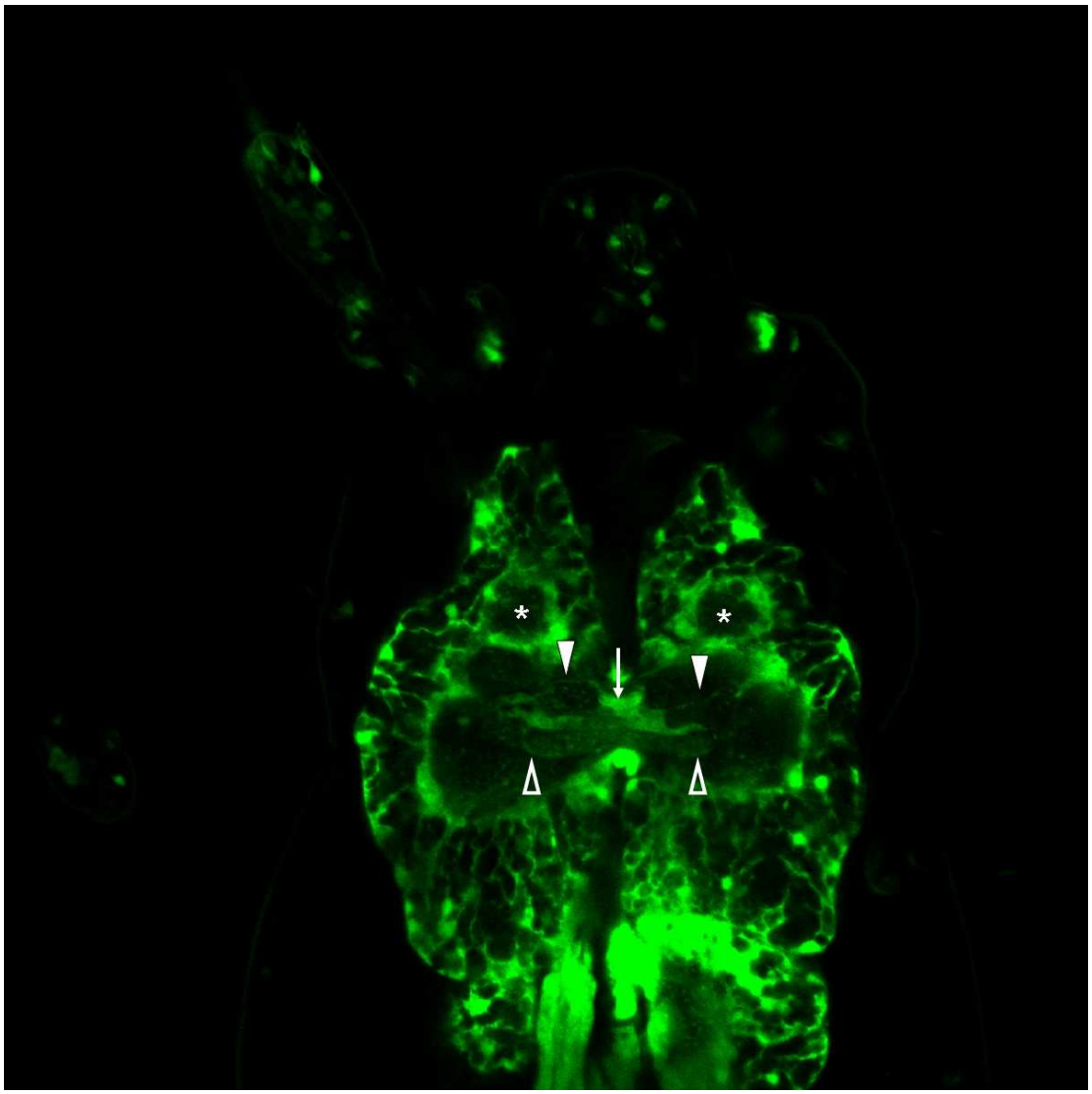

Fig. 7: Ectopic glia between the separated median lobes of the mushroom body in *Pax6* knockdown 3XP3-EGFP transgenic larva.

The green signal represents the EGFP expression. The white arrowheads mark the separated median lobes of the MSB. The white arrow marks the ectopic glia. The open arrowheads mark the CB. The asterisks mark the AL.

Abbreviations: pc: protocerebrum; AL: antennal lobe; MSB: mushroom body; CB: central body.

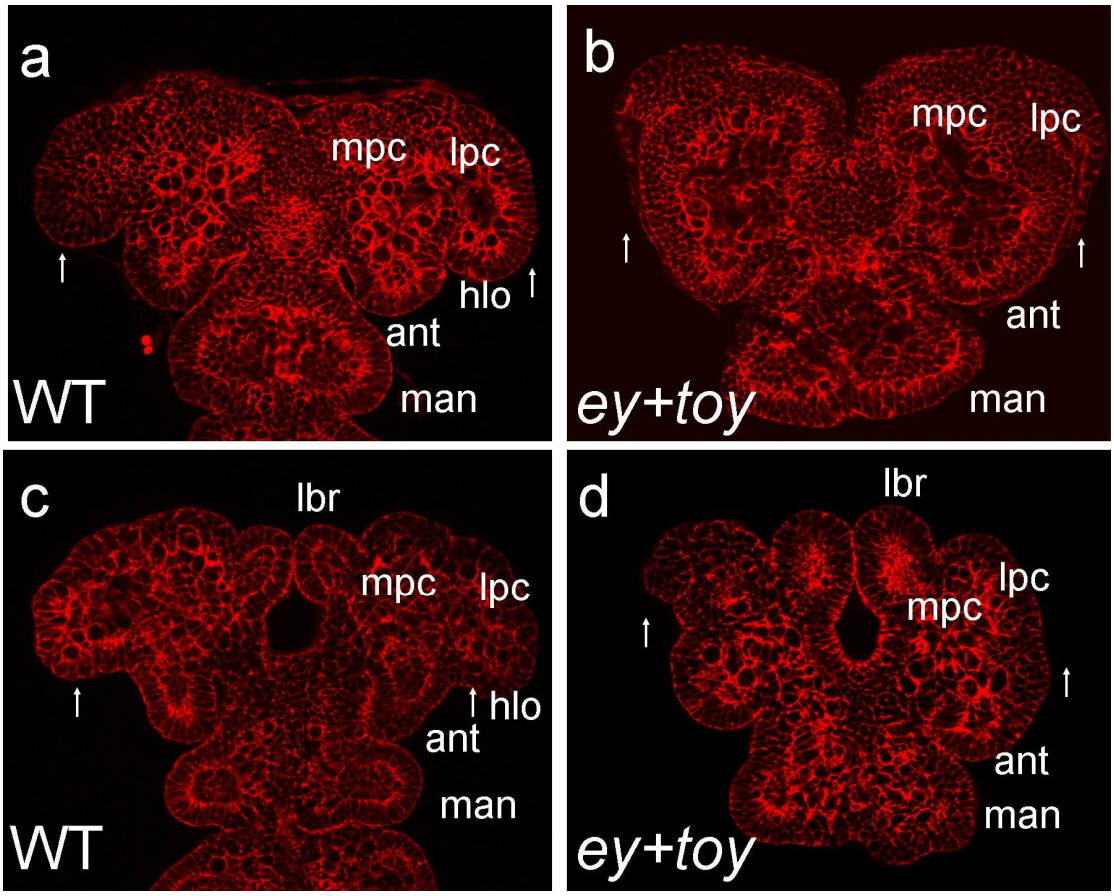

Fig. 8: Cellular organization of the early developing head in *Pax6* knockdown embryos.

(a-d) Alexa Fluor 633-phalloidin-labeled embryos. The red signal represents the Alexa Fluor 633 signal. (a, b) Late germband extension stage. (c, d) Germband extension complete stage. The arrows indicate the expanding head lobes, which were missing in the *Pax6* KD embryos (b, d).

Abbreviations: man: mandible; ant: antenna; lbr: labrum; lpc: lateral procephalon; hlo: head lobe; mpc: medial procephalon.

system (Fig. 8a). Posterior of the procephalic compartment, antennal and gnathal appendages have become defined as discrete bud-like tissue extensions. In *Pax6* KD embryos at late germband extension stage, the morphology of the initiating antennal and gnathal appendages was indistinguishable from that of WT embryos (Fig. 8b). However, the head lobe areas appeared less defined and relatively reduced and failed to expand, resulting in a characteristically triangular shape of the embryonic head (Fig. 8b).

After completion of germband extension in WT embryos, antennal and gnathal appendages have further extended and the lateral procephalon has expanded (Fig. 8c). In addition, the appendage-like bilateral anlagen of the labrum have formed as hallmark structures of this stage at the anterior median head (Fig. 8c). *Pax6* KD embryos possessed defined labral, antennal and gnathal appendages, but the head lobes appeared to be partially to completely reduced (Fig. 8d). These lateral procephalon defects persisted into subsequent stages (not shown), while the development of the labrum and antennal segment were not affected. Taken together, these findings suggested the complete failure of head lobe development as the cause for the lack of the derivative structures in the L1 head of strongly phenotypic *Pax6* KD animals.

3.5. Pax6 knockdown does not dramatically affect proliferation and cell death in the early embryonic head

To further explore the cellular cause of the missing head lobe extension, we examined *Pax6* KD embryos for the distribution and frequency of mitotic and apoptotic

cells, which were identified based on the morphology of propidium iodide-labeled cell nuclei. In the head of WT embryos at germband extension stage, dividing cells were scattered evenly across the entire embryonic head area (Fig. 9a). A similar number and distribution of dividing cells were observed in the *Pax6* KD embryonic head (Fig. 9b). Attempts to count dividing cells in embryos did not reveal a dramatic difference in *Pax6* KD embryos compared with WT (Table 3), suggesting that proliferation was not drastically affected by the depletion of *Pax6*.

Judging by the occurrence of fragmented nuclear morphologies, apoptotic cells were similarly dispersed in *Pax6* KD and WT embryos (Fig. 9c and d). In combination, these observations suggested that the lack of head lobe development in the *Pax6* KD animals was due neither to reduced proliferation nor increased apoptosis but to a lack of precursor specification.

3.6. Pax6 knockdown embryos lack the expression domains of wingless that partition the protocerebral neuroectoderm

The morphogenetic and cellular analysis of the embryonic *Pax6* KD head phenotype localized the KD-affected tissue region to the anterior lateral procephalon and established a morphological onset of the phenotype by the late germband extension stage. To confirm this diagnosis and obtain insights at the level of patterning, we investigated the expression of the signaling gene *wingless* (*wg*), which represents an informative marker of anterior embryonic head organization. As previously described(Liu et al., 2006), the earliest expression domains of *wg*, the protocerebral

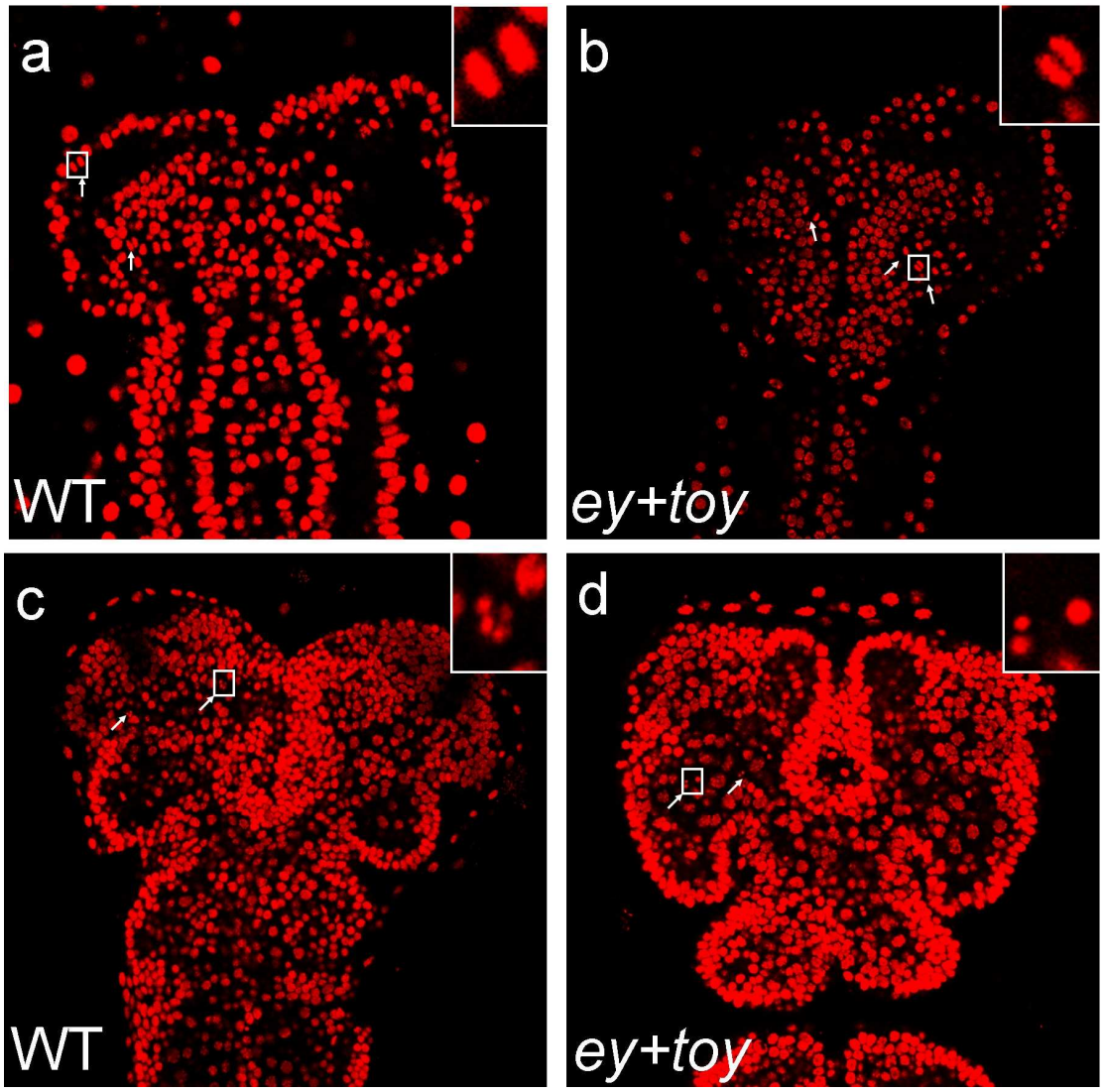

Fig. 9: Mitotic and apoptotic cells in *Pax6* knockdown embryos.

(a-d) Propidium iodide-labeled embryos. The red signal represents propidium iodide. (a, b) Proliferating cells in embryos at early germband extension stage. The arrows indicate dividing nuclei. (c, d) Apoptotic cells in embryos at late germband extension stage. The arrows indicate fragmented nuclei. The corner insets are enlargements of the box in each panel and indicate representative dividing (a, b) or apoptotic (c, d) nuclei.

Dividing nuclei counting			
	Pax6 KD-1	Pax6 KD-2	WT-1
lpc	12	10	7
mpc	2	5	1
ant	5	4	4
Apoptotic nuclei counting			
	Pax6 KD-3	WT-2	
pc	4	4	

Table 3: Number of dividing and apoptotic cells in propidium iodide-stained embryos.

Abbreviation: lpc: lateral procephalon; mpc: medial procephalon; ant: antenna; pc: procephalon.

neuroectoderm (pne) domains, are segmentation-like lateral stripes that mark a border between the antennal segment and the anterior procephalon on each side of the embryonic head (Fig. 10a1). During germband extension, the pne domains become more compact (Fig. 10b1 and 10c1). At the late germband extension stage, the pne domains disintegrate into three neuroblast precursor domains associated with the dorsal protocerebral neuroectoderm (dpn), the medial protocerebral neuroectoderm (mpn) and the ventral protocerebral neuroectoderm (vpn) (Fig. 10d1-f1). All of these domains contribute to the protocerebrum in the supraesophageal ganglion.

In *Pax6* KD embryos, the early *wg* pne domains appeared not dramatically affected in early germband (Fig. 10a2 and b2). However, at the middle germband extension stage procephalic expression of *wg* in *Pax6* KD embryos exhibited massive reduction, especially in the antennal expression domains which were notably restricted to peripheral tissue (compare Fig. 10c1 with c2). In subsequent stages, the reduced pne domain failed to divide into derivative domains, remaining intact throughout germband extension and retraction (Fig. 10d2-f2). The expression of *wg* in the labrum, antenna, intercalary and mandible segments was not affected in any of the *Pax6* KD embryos examined, consistent with the normal development of these structures in *Pax6* KD larvae.

The specific reduction and modification of the *wg* pne domain was consistent with the model that KD of *Pax6* results in an early perturbance of patterning in the anterior embryonic head. Moreover, the lack of the dpn, vpn and mpn domains suggested the development of the embryonic head compartments within and peripheral to these

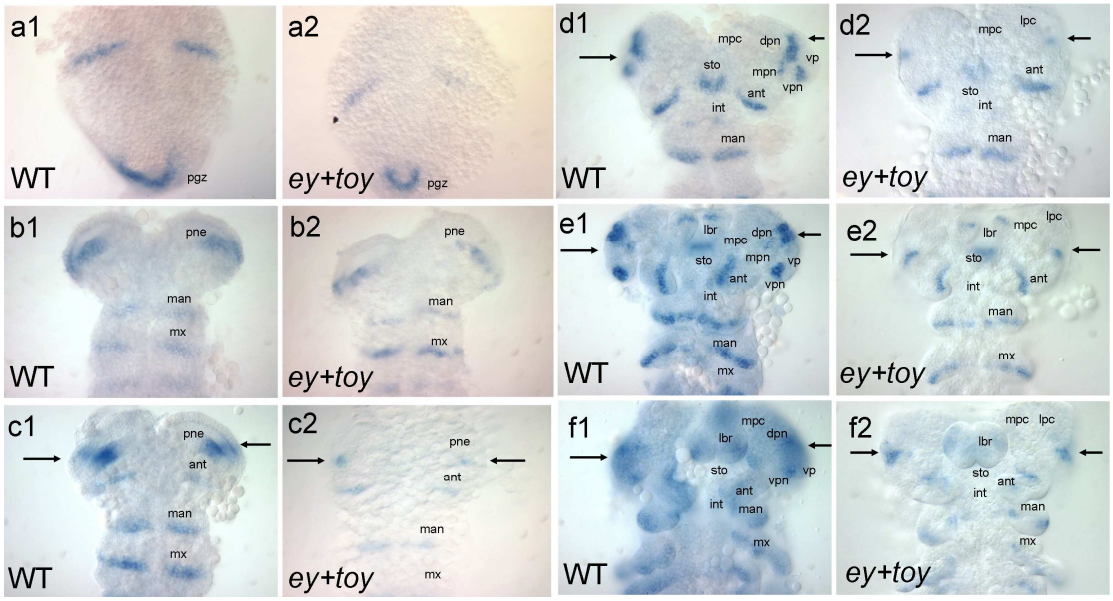

Fig. 10: *wingless* (*wg*) expression in the early developing head in *Pax6* knockdown embryos.

Ventral view of embryos labeled by whole mount *in situ* hybridization for *wg*. Anterior is to the top. The arrow indicates the *wg* expression domain in the procephalon. (a) Early blastoderm stage. (b) Early germband extension stage. (c) Middle germband extension stage. (d) Late germband extension stage. (e) Germband extension complete. (h) Germband retraction. The arrows indicate the procephalon.

Abbreviations: pgz: posterior growth zone; pne: protocerebral neuroectoderm; man: mandible; mx: maxilla; ant: antenna; sto: stomodeum; int: intercalary; dpn: dorsal protocerebral neuroectoderm; mpn: medial protocerebral neuroectoderm; vpn: ventral protocerebral neuroectoderm; vp: visual primordium; lbr: labrum; pc: procephalon; hlo: head lobe; mpc: medial procephalon.

domains, which includes the visual system and part of the protocerebrum, failed to be initiated in the *Pax6* KD animals.

3.7. Pax6 knockdown deletes marker gene expression in the lateral embryonic procephalon

To determine the spatial boundaries of the *Pax6*-contingent lateral procephalon in further detail, we examined the expression pattern of a panel of marker genes in *Pax6* KD embryos. This included the zinc finger transcription factor *disconnected* (*disco*) (Patel et al., 2007), which is specifically expressed in the early visual primordium of the *Tribolium* embryonic head at the beginning of early germband extension (Fig. 11a1). As the germband elongates, the expression of *disco* persists in the developing visual primordium and also initiates in the medial portions of all appendages including mandibles and antennae (Fig. 11b1 and c1). In *Pax6* KD embryos, *disco* expression was strongly reduced or depleted in the lateral procephalon, but not in any other domains (Fig. 11a2-c2). This result confirmed the specific depletion of the visual primordium as part of the lateral procephalon in *Pax6* KD embryos and explains the high penetrance of larval eye depletion in *Pax6* KD L1 larvae.

To further test whether neuroectoderm specification was affected by *Pax6* down-regulation in the lateral procephalon, we investigated the expression of the homeodomain transcription factor *intermediate neuroblast defective* (*ind*) (Wheeler et al., 2005). In *Drosophila*, the precursor cells of the inner optic lobe are characterized by *ind* expression. In *Tribolium*, *ind* is expressed in a candidate patch of inner optic lobe

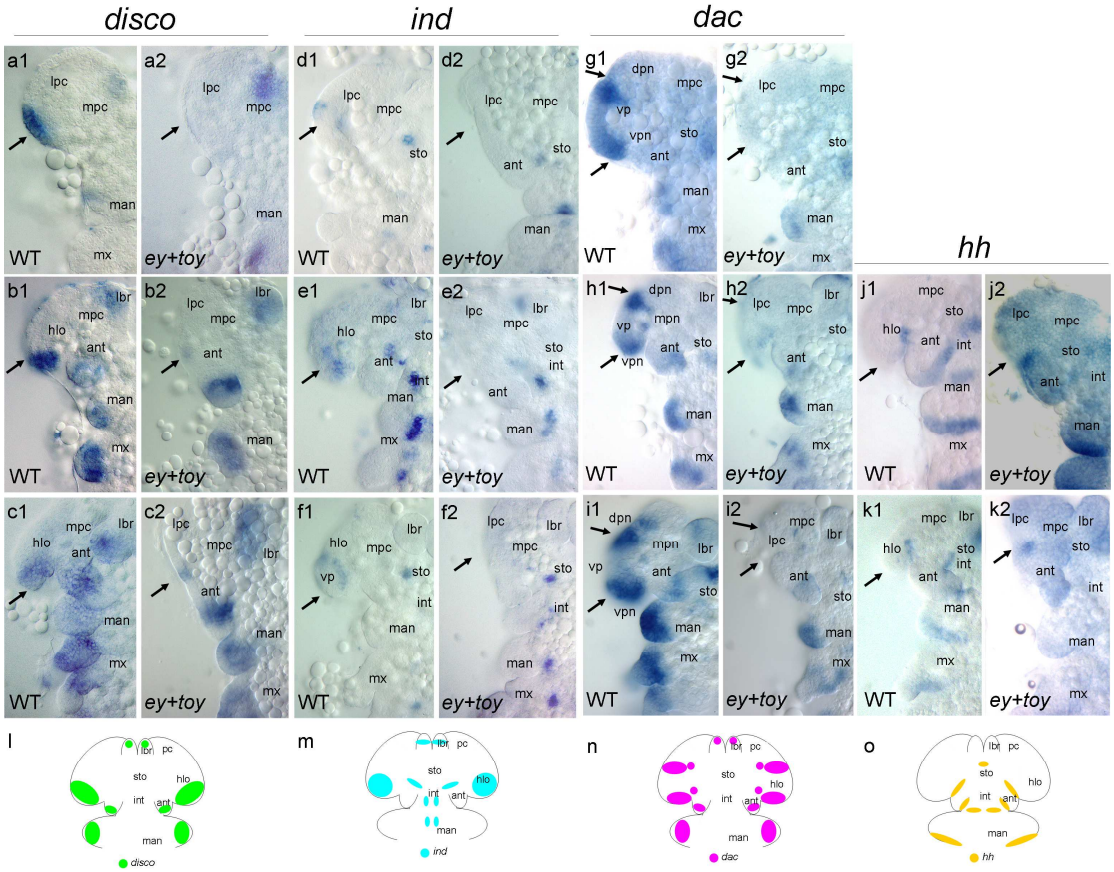

Fig. 11: Marker gene analysis of the developing head in *Pax6* knockdown embryos.

Ventral view of embryos labeled by whole mount *in situ* hybridization. Anterior is to the top. (a-c) *disco* expression in the early germband extension stage (a), germband extension complete stage (b) and germband retraction stage (c). The arrow indicates the lateral procephalon (a) or head lobe (b, c), which are marked by the expression of *disco*. (d-f) *ind* expression in the late germband extension stage (d), germband extension complete stage (e) and germband retraction stage (f). The arrow indicates the lateral procephalon (d) or head lobe (e, f), which are marked by the expression of *ind* in the intermediate column. (g-i) *dac* expression in middle germband extension stage (g), germband extension complete stage (h) and germband retraction stage (i). The arrows indicate *dac* expression within the procephalon. (j-k) *hh* expression in the late germband extension stage (j) and early germband retraction stage (k). The arrow indicates the head lobe (j, k), which is marked by *hh* at the posterior boundary. (l-o) Schematic view of marker gene expression in WT embryos at late germband extension stage.

Abbreviations: pne: protocerebral neuroectoderm; man: mandible; mx: maxilla; ant: antenna; sto: stomodeum; int: intercalary; dpn: dorsal protocerebral neuroectoderm; mpn: medial protocerebral neuroectoderm; vpn: ventral protocerebral neuroectoderm; vp: visual primordium; lbr: labrum; pc: procephalon; hlo: head lobe; mpc: medial procephalon.

precursor cells in the head lobe periphery (Fig. 11d1-f1). In addition, *ind* is expressed in neuroblast populations of both procephalic and gnathal head segments. In *Pax6* KD embryos, *ind* domain was specifically missing in the lateral procephalon (Fig. 11d2-f2), consistent with the absence of the entire visual anlagen as based on the lack of *disco* expression.

Next, we probed the expression of the transcription factor gene *dachshund* (*dac*) (Yang et al., 2009b), which starts to be expressed in two domains of the lateral embryonic procephalon during early germband extension (Fig. 11g1). The anterior domain is believed to contribute to the MSB, while the posterior domain is associated with part of the visual primordium (Posnien et al., 2011; Yang et al., 2009b). In *Pax6* KD embryos, these *dac* expression domains were generally highly reduced or completely absent (Fig. 11g2-i2), while the expression of *dac* in the antenna, intercalary and mandible segments was not conspicuously altered. The same pattern of select *dac* expression domain depletion was observed at later embryonic stages (Fig. 11i2). This finding supports the lack of lateral procephalon specification model inferred from the analysis of *wg* expression.

Segmentation-like expression of the signaling factor *hedgehog* (*hh*) (Farzana and Brown, 2008) marks the posterior boundary of embryonic segments, including the presumptive procephalon and the antennal segment (Fig. 11j and k). As the germband elongates, *hh* expression remains prominent at the boundaries separating the anterior procephalon from the antennal segment as well as the antennal segment from the intercalary segment (Fig. 11j1 and k1). In *Pax6* KD embryos, the *hh* expression domain

at the head lobe/antenna boundary was largely reduced or lost, while other expression domains were normal (Fig. 11j2 and k2), demonstrating that the extension of the head lobe was partially or completely disrupted.

Chapter 4: Discussion

4.1. Pax6: functions as a regional patterning gene in the early Tribolium head

Pax6 KD in the larvae of *Tribolium castaneum* leads to defects in the formation of the head capsule and supraesophageal ganglion in addition to the larval eye depletion. By analyzing a large sample of sensillum phenotypes, we outlined the region that is sensitive to *Pax6* level reduction. This region is located at the lateral and posterior margin of the dorsal larval head. These areas develop from the lateral procephalon of the embryo, which becomes morphologically distinct as the head lobes during germband extension and express *ey* and *toy* in broad and overlapping patterns (Fig. 1) (Yang et al., 2009a). In normal embryos, the lateral procephalon extends posteriorly along the antenna and forms the head lobe during late germband extension stage. The posterior head lobe subsequently gives rise to the larval eyes and the anterior head lobe develops into the larval protocerebrum (Liu et al., 2006). In *Pax6* KD embryos, the lateral procephalon failed to extend and form the head lobe. We therefore conclude that the loss of the head lobes is the cause of the reduction in the lateral head capsule and depletion of the larval eyes in the L1 larvae. This was also

supported by the reduction of head lobe-derived elements of the supraesophageal ganglion like the MSB in *Pax6* KD L1 larvae.

To understand the cause of failing embryonic head lobe development, we examined cell proliferation, apoptosis and marker gene expression in early embryonic *Pax6* KD specimens. Neither aberrant proliferation nor cell death patterns were observed in the *Pax6* KD embryos. The most informative observation was the impact of *Pax6* KD on *wg* expression. Instead of partitioning into vpn, mpn and dpn domains, the *wg* pne expression domain subsisted as a relict domain in the lateral embryonic head. This finding is significant given the earlier proposal that the partitioning of the pne into its subdomain derivatives represents the non-segmental origin of the head lobe compartments (Liu et al., 2006). Further consistent with this interpretation of the *Pax6* KD embryos, head lobe-specific expression domains of *disco*, *dac* and *ind* were partially or completely missing in the *Pax6* KD embryos. Considering the consistent evidence of a compartment-wide effect of *Pax6* KD in the *Tribolium* embryonic head, we further conclude that *Pax6* acts as a regional patterning gene that specifies the fate of the lateral procephalon during early embryonic development.

4.2. Comparison of Pax6 function in other species

In *small eye* mutant mice, the nasal cavity is not formed properly in addition to eye defects, indicating disruption of nasal epithelium development (Hill et al., 1991; Hogan et al., 1986). Both eye and nasal cavities develop from the embryonic ectodermal placodes and *Pax6* has been shown to function as an essential early

differentiation factor in these placodes (Grindley et al., 1995). Further studies in mouse and rat revealed that *Pax6* mutants suffer from defects in tooth and facial skeleton formation, expanding the *Pax6*-dependent region to the cephalic ectodermal patterning center and subsequent craniofacial region in vertebrates (Compagnucci et al., 2011; Kriangkrai et al., 2006; Quinn et al., 1997).

Pax6 has been found to be expressed in the CNS of almost all examined organisms, even in organisms which do not have *Pax6* expression in the visual organ (Martin-Duran et al., 2012). In mouse, *Pax6* is broadly expressed in the developing brain (Walther and Gruss, 1991). Comparative studies revealed a common origin of the invertebrate MSB and the vertebrate pallium (Tomer et al., 2010). Intriguingly, *Pax6* was found to be expressed and required in both cerebral structures (Callaerts et al., 2001; Furukubo-Tokunaga et al., 2009; Gotz et al., 1998; Posnien et al., 2011; Warren et al., 1999), further confirming the regulatory and functional conservation of *Pax6* genes.

Although *Pax6* is required for the normal function of various brain compartments (Engelkamp et al., 1999; Mastick et al., 1997; Osumi et al., 1997; Stoykova et al., 1996; Warren and Price, 1997), it is not the earliest marker or an essential determinant of murine neuroectoderm specification (Zhang et al., 2010). In primates, however, *Pax6* was found to be the determinant of neuroectoderm (Zhang et al., 2010). In *Tribolium*, our data reveal that *Pax6* is required for proper development of the larval CNS. Considering the early expression pattern of *Pax6* genes (Yang et al., 2009a) and the remaining *wg* expression domain in the *Pax6* KD embryos, it is unlikely that *Pax6*

genes are the determinant of the neuroectoderm in *Tribolium*. Despite defective neuropils, the glia of the supraesophageal ganglion did not display any obvious deficiency, indicating that the fate of neuroectoderm was properly initiated and that the development of the glia was not affected by *Pax6* depletion. Consistently, *ey* was found to be expressed only in the neurons, but not the surrounding neuropil glia cells in *Drosophila* (Callaerts et al., 2001). In vertebrates, however, *Pax6* is also expressed in the glia.

3. Compartmental organization of the anterior procephalon

The lateral head cuticle is believed to be formed from the embryonic procephalon by folding and fusion, leaving a Y-shaped epicranial suture as evidence of this process (Posnien et al., 2010). The suture is therefore also considered a morphological landmark of the boundary of the ocular compartment and the labral compartment, which are derived from the procephalon and labrum, respectively. In the most severely affected cases of *Pax6* KD larvae, a 'neck'-like groove was formed spanning the width of the entire posterior dorsal head (Fig 2d). This groove, intriguingly, is located within the ocular compartment and separates the ocular compartment into anterior and posterior halves. This finding leads to the hypothesis that an intracompartmental boundary might exist within the procephalon and the two putative anterior and posterior halves might have different identities and developmental origins.

Consistent with this idea, all *Pax6* KD affected sensilla were in the anterior half of the ocular compartment. The only element located in the posterior half, the bell row, which is composed of five alveoli, was rarely missing (Fig 4c), although the arrangement of the five alveoli varied. Considering the early blastoderm expression of *ey* and *toy* (Yang et al., 2009a), their lateral expression patterns seems to form before segmentation is established, suggesting that they are not regulated by segmentation signals. However, the expression domains of *ey* and *toy* do not extend into the anterior-most or the medial procephalon (Yang et al., 2009a). In contrast to the impaired structures derived from the lateral procephalon, the unaffected CB in the *Pax6* KD larvae implies a different identity within the procephalon. In *Six3* KD larvae, the medial procephalon, which contributes to the CB, loses its identity and molecular markers of the lateral procephalon expand medially (Posnien et al., 2011). This observation suggests that the fate of the median procephalon, defined by *Six3*, is different from the lateral procephalon, which is defined by *Pax6*. This idea is also consistent with the relative phenotypic independence of the closely adjacent CB and MSB.

4. The impact of Pax6 on neighboring compartments

The anterior and medial vertex, which are outlined at the anterior and medial side of the Y-shaped epicranial suture, are derived from the labrum (Posnien et al., 2010). In the presence analysis of the sensillum pattern, no abnormality was found in the elements that lay in the anterior and medial vertex (Fig. 4c). However, the medial

vertical elements were often found duplicated or transformed (KD 98.3% vs. control 0%), while the anterior vertical elements were not affected.

Of further note, the medial vertex adjacent to the ocular compartment also exhibited evidence of being affected in *Pax6* KD larvae. However, the anterior vertex, which is derived from the labrum, but not directly connected with the ocular compartment, was found to be unaffected. Given that the sensilla are peripheral sensory organs, it is possible that compensatory mechanisms exist to maintain a specific density of sensilla in the dorsal cuticle. Considering the finding that homeodomain proteins can be secreted and function as signaling molecules (Chatelin et al., 1996) and that *Pax6* has been found to function in this non- autonomous manner in zebrafish (Lesaffre et al., 2007), it is tempting to speculate that the *Tribolium* PAX6 proteins have the potential to function beyond their mRNA expression domains and into neighboring regions.

REFERENCES

Ashery-Padan, R., Zhou, X., Marquardt, T., Herrera, P., Toube, L., Berry, A., and Gruss, P. (2004). Conditional inactivation of Pax6 in the pancreas causes early onset of diabetes. Dev Biol 269, 479-488.

Bopp, D., Burri, M., Baumgartner, S., Frigerio, G., and Noll, M. (1986). Conservation of a large protein domain in the segmentation gene paired and in functionally related genes of Drosophila. Cell 47, 1033-1040.

Bucher, G., Scholten, J., and Klingler, M. (2002). Parental RNAi in Tribolium (Coleoptera). Curr Biol 12, R85-86.

Callaerts, P., Clements, J., Francis, C., and Hens, K. (2006). Pax6 and eye development in Arthropoda. Arthropod Struct Dev 35, 379-391.

Callaerts, P., Halder, G., and Gehring, W.J. (1997). PAX-6 in development and evolution. Annu Rev Neurosci 20, 483-532.

Callaerts, P., Leng, S., Clements, J., Benassayag, C., Cribbs, D., Kang, Y.Y., Walldorf, U., Fischbach, K.F., and Strauss, R. (2001). Drosophila Pax-6/eyeless is essential for normal adult brain structure and function. J Neurobiol 46, 73-88.

Chatelin, L., Volovitch, M., Joliot, A.H., Perez, F., and Prochiantz, A. (1996). Transcription factor hoxa-5 is taken up by cells in culture and conveyed to their nuclei. Mech Dev 55, 111-117.

Chow, R.L., Altmann, C.R., Lang, R.A., and Hemmati-Brivanlou, A. (1999). Pax6 induces ectopic eyes in a vertebrate. Development 126, 4213-4222.

Clements, J., Hens, K., Francis, C., Schellens, A., and Callaerts, P. (2008). Conserved role for the Drosophila Pax6 homolog Eyeless in differentiation and function of insulin-producing neurons. Proc Natl Acad Sci U S A 105, 16183-16188.

Compagnucci, C., Fish, J.L., Schwark, M., Tarabykin, V., and Depew, M.J. (2011). Pax6 regulates craniofacial form through its control of an essential cephalic ectodermal patterning center. Genesis 49, 307-325.

Czerny, T., Halder, G., Kloter, U., Souabni, A., Gehring, W.J., and Busslinger, M. (1999). twin of eyeless, a second Pax-6 gene of Drosophila, acts upstream of eyeless in the control of eye development. Mol Cell 3, 297-307.

Engelkamp, D., Rashbass, P., Seawright, A., and van Heyningen, V. (1999). Role of Pax6 in development of the cerebellar system. Development 126, 3585-3596.

Farzana, L., and Brown, S.J. (2008). Hedgehog signaling pathway function conserved in Tribolium segmentation. Dev Genes Evol 218, 181-192.

Friedrich, M., and Benzer, S. (2000). Divergent decapentaplegic expression patterns in compound eye development and the evolution of insect metamorphosis. J Exp Zool 288, 39-55.

Furukubo-Tokunaga, K., Adachi, Y., Kurusu, M., and Walldorf, U. (2009). Brain patterning defects caused by mutations of the twin of eyeless gene in Drosophila melanogaster. Fly (Austin) 3, 263-269.

Gotz, M., Stoykova, A., and Gruss, P. (1998). Pax6 controls radial glia differentiation in the cerebral cortex. Neuron 21, 1031-1044.

Grindley, J.C., Davidson, D.R., and Hill, R.E. (1995). The role of Pax-6 in eye and nasal development. Development 121, 1433-1442.

Halder, G., Callaerts, P., and Gehring, W.J. (1995). Induction of ectopic eyes by targeted expression of the eyeless gene in Drosophila. Science 267, 1788-1792.

Hanson, I.M. (2003). PAX6 and congenital eye malformations. Pediatr Res 54, 791-796.

Hauck, B., Gehring, W.J., and Walldorf, U. (1999). Functional analysis of an eye specific enhancer of the eyeless gene in Drosophila. Proc Natl Acad Sci U S A 96, 564-569.

Hill, R.E., Favor, J., Hogan, B.L., Ton, C.C., Saunders, G.F., Hanson, I.M., Prosser, J., Jordan, T., Hastie, N.D., and van Heyningen, V. (1991). Mouse small eye results from mutations in a paired-like homeobox-containing gene. Nature 354, 522-525.

Hogan, B.L., Horsburgh, G., Cohen, J., Hetherington, C.M., Fisher, G., and Lyon, M.F. (1986). Small eyes (Sey): a homozygous lethal mutation on chromosome 2 which affects the differentiation of both lens and nasal placodes in the mouse. J Embryol Exp Morphol 97, 95-110.

Kriangkrai, R., Chareonvit, S., Yahagi, K., Fujiwara, M., Eto, K., and Iseki, S. (2006). Study of Pax6 mutant rat revealed the association between upper incisor formation and midface formation. Dev Dyn 235, 2134-2143.

Kronhamn, J., Frei, E., Daube, M., Jiao, R., Shi, Y., Noll, M., and Rasmuson-Lestander, A. (2002). Headless flies produced by mutations in the paralogous Pax6 genes eyeless and twin of eyeless. Development 129, 1015-1026.

Kurusu, M., Nagao, T., Walldorf, U., Flister, S., Gehring, W.J., and Furukubo-Tokunaga, K. (2000). Genetic control of development of the mushroom bodies, the associative learning centers in the Drosophila brain, by the eyeless, twin of eyeless, and Dachshund genes. Proc Natl Acad Sci U S A 97, 2140-2144.

Lesaffre, B., Joliot, A., Prochiantz, A., and Volovitch, M. (2007). Direct non-cell autonomous Pax6 activity regulates eye development in the zebrafish. Neural Dev 2, 2.

Liu, Z., and Friedrich, M. (2004). The Tribolium homologue of glass and the evolution of insect larval eyes. Dev Biol 269, 36-54.

Liu, Z., Yang, X., Dong, Y., and Friedrich, M. (2006). Tracking down the "head blob": comparative analysis of wingless expression in the developing insect procephalon reveals progressive reduction of embryonic visual system patterning in higher insects. Arthropod Struct Dev 35, 341-356.

Lorenzen, M.D., Berghammer, A.J., Brown, S.J., Denell, R.E., Klingler, M., and Beeman, R.W. (2003). piggyBac-mediated germline transformation in the beetle Tribolium castaneum. Insect Mol Biol 12, 433-440.

Martin-Duran, J.M., Monjo, F., and Romero, R. (2012). Morphological and molecular development of the eyes during embryogenesis of the freshwater planarian Schmidtea polychroa. Dev Genes Evol 222, 45-54.

Mastick, G.S., Davis, N.M., Andrew, G.L., and Easter, S.S., Jr. (1997). Pax-6 functions in boundary formation and axon guidance in the embryonic mouse forebrain. Development 124, 1985-1997.

Niederfuhr, A., Hummerich, H., Gawin, B., Boyle, S., Little, P.F., and Gessler, M. (1998). A sequence-ready 3-Mb PAC contig covering 16 breakpoints of the Wilms tumor/anirida region of human chromosome 11p13. Genomics 53, 155-163.

Osumi, N., Hirota, A., Ohuchi, H., Nakafuku, M., Iimura, T., Kuratani, S., Fujiwara, M., Noji, S., and Eto, K. (1997). Pax-6 is involved in the specification of hindbrain motor neuron subtype. Development 124, 2961-2972.

Patel, M., Farzana, L., Robertson, L.K., Hutchinson, J., Grubbs, N., Shepherd, M.N., and Mahaffey, J.W. (2007). The appendage role of insect disco genes and possible implications on the evolution of the maggot larval form. Dev Biol 309, 56-69.

Pavlopoulos, A., Berghammer, A.J., Averof, M., and Klingler, M. (2004). Efficient transformation of the beetle Tribolium castaneum using the Minos transposable element: quantitative and qualitative analysis of genomic integration events. Genetics 167, 737-746.

Posnien, N., and Bucher, G. (2010). Formation of the insect head involves lateral contribution of the intercalary segment, which depends on Tc-labial function. Dev Biol 338, 107-116.

Posnien, N., Koniszewski, N.D., Hein, H.J., and Bucher, G. (2011). Candidate gene screen in the red flour beetle Tribolium reveals six3 as ancient regulator of anterior median head and central complex development. PLoS Genet 7, e1002416.

Posnien, N., Schinko, J., Grossmann, D., Shippy, T.D., Konopova, B., and Bucher, G. (2009). RNAi in the red flour beetle (Tribolium). Cold Spring Harb Protoc 2009, pdb prot5256.

Posnien, N., Schinko, J.B., Kittelmann, S., and Bucher, G. (2010). Genetics, development and composition of the insect head--a beetle's view. Arthropod Struct Dev 39, 399-410.

Quinn, J.C., West, J.D., and Kaufman, M.H. (1997). Genetic background effects on dental and other craniofacial abnormalities in homozygous small eye (Pax6Sey/Pax6Sey) mice. Anat Embryol (Berl) 196, 311-321.

Quiring, R., Walldorf, U., Kloter, U., and Gehring, W.J. (1994). Homology of the eyeless gene of Drosophila to the Small eye gene in mice and Aniridia in humans. Science 265, 785-789.

Schinko, J.B., Kreuzer, N., Offen, N., Posnien, N., Wimmer, E.A., and Bucher, G. (2008). Divergent functions of orthodenticle, empty spiracles and buttonhead in early head patterning of the beetle Tribolium castaneum (Coleoptera). Dev Biol 317, 600-613.

Stoykova, A., Fritsch, R., Walther, C., and Gruss, P. (1996). Forebrain patterning defects in Small eye mutant mice. Development 122, 3453-3465.

Suzuki, T., and Saigo, K. (2000). Transcriptional regulation of atonal required for Drosophila larval eye development by concerted action of eyes absent, sine oculis and hedgehog signaling independent of fused kinase and cubitus interruptus. Development 127, 1531-1540.

Tomer, R., Denes, A.S., Tessmar-Raible, K., and Arendt, D. (2010). Profiling by image registration reveals common origin of annelid mushroom bodies and vertebrate pallium. Cell 142, 800-809.

Walther, C., and Gruss, P. (1991). Pax-6, a murine paired box gene, is expressed in the developing CNS. Development 113, 1435-1449.

Warren, N., Caric, D., Pratt, T., Clausen, J.A., Asavaritikrai, P., Mason, J.O., Hill, R.E., and Price, D.J. (1999). The transcription factor, Pax6, is required for cell proliferation and differentiation in the developing cerebral cortex. Cereb Cortex 9, 627-635.

Warren, N., and Price, D.J. (1997). Roles of Pax-6 in murine diencephalic development. Development 124, 1573-1582.

Wheeler, S.R., Carrico, M.L., Wilson, B.A., and Skeath, J.B. (2005). The Tribolium columnar genes reveal conservation and plasticity in neural precursor patterning along the embryonic dorsal-ventral axis. Dev Biol 279, 491-500.

Xu, P.X., Zhang, X., Heaney, S., Yoon, A., Michelson, A.M., and Maas, R.L. (1999). Regulation of Pax6 expression is conserved between mice and flies. Development 126, 383-395.

Yang, X., Weber, M., Zarinkamar, N., Posnien, N., Friedrich, F., Wigand, B., Beutel, R., Damen, W.G., Bucher, G., Klingler, M., et al. (2009a). Probing the Drosophila retinal determination gene network in Tribolium (II): The Pax6 genes eyeless and twin of eyeless. Dev Biol 333, 215-227.

Yang, X., Zarinkamar, N., Bao, R., and Friedrich, M. (2009b). Probing the Drosophila retinal determination gene network in Tribolium (I): The early retinal genes dachshund, eyes absent and sine oculis. Dev Biol 333, 202-214.

Zhang, X., Huang, C.T., Chen, J., Pankratz, M.T., Xi, J., Li, J., Yang, Y., Lavaute, T.M., Li, X.J., Ayala, M., et al. (2010). Pax6 is a human neuroectoderm cell fate determinant. Cell Stem Cell 7, 90-100.

ABTRACT

PAX6 IS REQUIRED FOR THE DEVELOPMENT OF THE LATERAL PROCEPHALON IN TRIBOLIUM

by

QING LUAN

August 2012

Advisor: Dr. Markus Friedrich

Major: Biological Sciences

Degree: Master of Science

In *Tribolium*, combinatorial knockdown of the *Pax6* orthologs *eyeless* (*ey*) and *twin of eyeless* (*toy*) affects the peripheral visual system but also other areas of the dorsal larval head capsule. To elucidate the role of *Pax6* genes during *Tribolium* embryonic head development in detail, we performed an extensive analysis of cuticle elements, brain anatomy, embryonic head morphogenesis and developmental marker gene expression. Our results reveal that *Pax6* is required for the development of a large contiguous area of the lateral anterior head, morphologically addressed as the embryonic head lobes, which encompass the neuroectodermal precursor tissues of the visual system, parts of the mushroom bodies, and the dorsal head cuticle. In addition to consolidating our understanding of the developmental compartmentalization of the early *Tribolium* head, these data characterize *Pax6* genes as regional regulators of development.

AUTOBIOGRAPHICAL STATEMENT

I was born 27 years ago in Tianjin, China. As the only child in my family, I grew up with comprehensive care and love from my parents. After 6 years of primary school, I enrolled at Yaohua High School, Tianjin, China, which provided a 1-year condensed high school curriculum to qualified students. While there, two events occurred that would crucially impact the rest of my life: first, I encountered a respectful teacher who taught me to think independently; second, I became obsessed with the natural sciences, especially biology. Based on my interest, I enrolled in the Biochemistry Department at Nanjing University, China in 2002.

After graduating with my bachelor's degree in 2006, I worked as a research assistant in biological labs for 3 years and accumulated much experience. In 2009, I was offered a position as a research scientist in the R&D Department of the Peteck Biotechnology Corporation. However, I found that I was still interested in pursuing further science education and applied to Wayne State University. Luckily, I was accepted into the Biological Sciences Department in the fall of 2010 and offered a Thomas C. Rumble Fellowship.

In summer 2011, two more crucial events occurred: first, I joined Dr. Friedrich's lab and started to work on my thesis project; second, I got married. I had a good time cooperating with Dr. Friedrich and his lab members and we made satisfying progress together. I will always treasure this experience as I move forward in my career track.